01 Jul 2019

Bioprinting with Human Stem Cell-Laden Alginate-Gelatin Bioink and Bioactive Glass for Tissue Engineering

Krishna C. R. Kolan

Julie A. Semon
Missouri University of Science and Technology, semonja@mst.edu

Bradley Bromet

D. E. Day
Missouri University of Science and Technology, day@mst.edu

et. al. For a complete list of authors, see https://scholarsmine.mst.edu/biosci_facwork/307

Recommended Citation

K. C. Kolan et al., "Bioprinting with Human Stem Cell-Laden Alginate-Gelatin Bioink and Bioactive Glass for Tissue Engineering," *International Journal of Bioprinting*, vol. 5, no. 2.2 Special Issue, pp. 3-15, Whioce Publishing Pte. Ltd., Jul 2019.
The definitive version is available at https://doi.org/10.18063/ijb.v5i2.2.204

RESEARCH ARTICLE

Bioprinting with human stem cell-laden alginate-gelatin bioink and bioactive glass for tissue engineering

Krishna C. R. Kolan[1]*, Julie A. Semon[2], Bradley Bromet[2], Delbert E. Day[3], Ming C. Leu[1]

[1]Department of Mechanical and Aerospace Engineering, Missouri University of Science and Technology, Rolla, Missouri, USA
[2]Department of Biological Sciences, Missouri University of Science and Technology, Rolla, Missouri, USA
[3]Department of Materials Science and Engineering, Missouri University of Science and Technology, Rolla, Missouri, USA

Abstract: Three-dimensional (3D) bioprinting technologies have shown great potential in the fabrication of 3D models for different human tissues. Stem cells are an attractive cell source in tissue engineering as they can be directed by material and environmental cues to differentiate into multiple cell types for tissue repair and regeneration. In this study, we investigate the viability of human adipose-derived mesenchymal stem cells (ASCs) in alginate-gelatin (Alg-Gel) hydrogel bioprinted with or without bioactive glass. Highly angiogenic borate bioactive glass (13-93B3) in 50 wt% is added to polycaprolactone (PCL) to fabricate scaffolds using a solvent-based extrusion 3D bioprinting technique. The fabricated scaffolds with 12 × 12 × 1 mm^3 in overall dimensions are physically characterized, and the glass dissolution from PCL/glass composite over a period of 28 days is studied. Alg-Gel composite hydrogel is used as a bioink to suspend ASCs, and scaffolds are then bioprinted in different configurations: Bioink only, PCL+bioink, and PCL/glass+bioink, to investigate ASC viability. The results indicate the feasibility of the solvent-based bioprinting process to fabricate 3D cellularized scaffolds with more than 80% viability on day 0. The decrease in viability after 7 days due to glass concentration and static culture conditions is discussed. The feasibility of modifying Alg-Gel with 13-93B3 glass for bioprinting is also investigated, and the results are discussed.

Keywords: Bioprinting; Alginate-gelatin bioink; Borate bioactive glass; Human adipose-derived stem cells Polymer/bioactive glass composite

*Correspondence to: Krishna C. R. Kolan, Department of Mechanical and Aerospace Engineering, Missouri University of Science and Technology, Rolla, Missouri, USA; kolank@mst.edu

Received: April 30, 2019; **Accepted:** May 28, 2019; **Published Online:** July 12, 2019

(This article belongs to the *Special Issue: Bioprinting in the Americas*)

Citation: Kolan KCR, Semon JA, Bromet B, *et al*., 2019, Bioprinting with human stem cell-laden alginate-gelatin bioink and bioactive glass for tissue engineering. *Int J Bioprint*, 5(2.2): 204. http://dx.doi.org/10.18063/ijb.v5i2.2.204

1. Introduction

Bioprinting has been a subject of interest for many researchers in the past decade, especially as it offers to create and investigate different tissue models *in vitro*. In the tissue engineering and regenerative medicine research community, bioprinting is referred to as computer-aided transfer processes for patterning and assembling living cells and non-living materials with a prescribed two-dimensional (2D) or three-dimensional (3D) organization to produce bio-engineered structures[1]. Although there is no official categorization of the available bioprinting techniques, they can be primarily classified into four categories: (i) Inkjet-based, (ii) extrusion-based, (iii) laser-assisted, and (iv) stereolithography-based. Extrusion-based bioprinting is by far the most successful and widely adopted technique due to its compatibility to use of high viscosity materials and a variety of hydrogels[2-4]. In extrusion-based bioprinting, melt-extrusion is one of the extensively adopted methods to fabricate porous support structure for depositing

bioinks. However, the disadvantage of this method is that polymers with relatively low melting point such as polycaprolactone (PCL) are used as a support structure in a majority of the studies[5]. This method requires high temperature (~100°C) to extrude even for PCL/glass composites with 50 wt% glass, making it unsuitable for bioprinting with the polymer composites. Hence, in the current work, we use a solvent-based extrusion bioprinting technique that enables printing with a variety of polymers as long as they can be dissolved in an organic solvent to form an extrudable paste[6,7].

In bioprinting, a majority of researchers still use immortal cell lines to characterize the process viability and demonstrate the functionality of the bioprinted structures. However, it is crucial to understand that the cell lines do not completely mimic primary cells, and the experiments should be duplicated with primary cells for a comprehensive conclusion[8]. There is a growing interest in utilizing stem cells and bioprinting techniques to create 3D cell cultures for stem cell research[9,10]. Mesenchymal stem cells (MSCs) have been used for cell therapy and tissue engineering due to their ability to differentiate into multiple mesenchymal and non-mesenchymal lineages and their immune modulatory effects[11]. The density and frequency of MSCs in adipose tissue are much higher than the more commonly used source of bone marrow, yielding 100-500 times more cells per tissue volume[12,13]. Despite having high therapeutic potential, ability to release angiogenic growth factors, and self-renewal ability, human adipose-derived mesenchymal stem cells (ASCs) have not been thoroughly investigated in bioprinting and 3D cell cultures[9,14].

In bioprinting, coculturing stem cells with tissue-specific cells and combining stem cells to create a composite bioink are a common practice to exploit benefits of stem cells in a bioprinted 3D environment for tissue engineering and regenerative medicine. For example, MSCs combined with chondrocytes and bioprinted for cartilage repair and replacement showed improved proliferative effect and production of type 2 collagen[15]. Another study reported that MSCs when combined with primary hepatocytes supported the long-term culture of hepatocytes in a 3D environment to aid artificial 3D liver model creation[16]. MSCs were combined with human umbilical vein endothelial cells to create thick vascularized tissues and mineralized bone tissues[17,18]. While the incorporation of growth factors such as the vascular endothelial growth factor (VEGF) and bone morphogenetic protein is the most common approach to engineer vascularized bone, very few researchers have utilized the effect of ionic micronutrients on bone formation in a 3D environment[19-21].

Bioactive glasses dissolve and release micronutrients such as calcium, potassium, and sodium to encourage new tissue growth. Bioactive borate glass (13-93B3) is different from the traditional silicate-based Bioglass® (45S5) as it reacts 10 times faster in comparison to 45S5 glass and even heals "difficult-to-heal" diabetic wounds without any external growth factors[22,23]. The 13-93B3 glass was approved in 2017 by the Food and Drug Administration in the United States for treating skin burns and chronic wounds with a trade name of Mirragen™ Advanced Wound Matrix[24]. The composition of this glass is provided in Table 1. The release of ions from 13-93B3 glass is thought to be the reason for its wound healing properties and being highly angiogenic[23,25]. In the current work, we characterized the bioactivity and 13-93B3 glass dissolution from PCL matrix and investigated the viability of ASCs suspended in alginate-gelatin (Alg-Gel) hydrogel and bioprinted in between PCL/13-93B3 glass filaments. We also explored the feasibility of direct addition of 13-93B3 glass to the Alg-Gel hydrogel as a bioink.

2. Materials and Methods

2.1 PCL and PCL/13-93B3 Pastes Preparation

For PCL paste preparation, 2 g of PCL powder (MW – 50,000 g/mol, Polysciences, Inc., Warrington, PA, USA) was added to 2.3 ml chloroform (Sigma-Aldrich, St. Louis, MO, USA) in a polypropylene tub, which is then centrifugally mixed for 5 min at 2500 RPM in a FlackTek SpeedMixer™ (Landrum, SC, USA). To prepare PCL/13-93B3 glass composite paste, 1.5 g of 13-93B3 glass (~20 µm particle size, MO-SCI Corporation, Rolla, MO, USA) is added to 2.3 ml chloroform and ultrasonicated for 3 min to remove any agglomerates followed by addition of 1.5 g of PCL powder (to achieve a 50:50 PCL/13-93B3 composite). The mixture is centrifugally mixed for 5 min at 2500 RPM in a SpeedMixer™. The pastes are transferred to 3 ml syringe barrels (Loctite® Henkel, Rocky Hill, CT, USA) attached with 25G or 250 µm internal diameter SmoothFlow Tapered tips (Nordson EFD, Westlake, OH, USA) before fabrication.

2.2 Cell Culture

Frozen vials of approximately 1×10^6 ASCs obtained from three separate donors (LaCell, New Orleans, LA) are thawed, plated on 150 cm^2 culture dishes (Nunc, Rochester, NY) in 25 ml complete culture media (CCM) and incubated at 37.5°C with 5% humidified CO_2. CCM consisted of 10% fetal bovine serum (Corning, Manassas, VA), alpha minimum essential media (α-MEM, Sigma-Aldrich, St. Louis, MO), 1% 100 L-glutamine (GE Life Sciences,

Table 1. Compositions (in wt%) of 13-93B3 glass compared to 45S5 Bioglass®.

Wt. (%)	SiO_2	Na_2O	K_2O	MgO	CaO	P_2O_5	B_2O_3
45S5	45	24.5	-	-	24.5	6	-
13-93B3	-	6	12	5	20	4	53

Logan, UT), and 1% ×100× antibiotic/antimycotic (GE Life Sciences, Logan, UT). After 24 h, the media are removed and adherent, viable cells are washed twice with phosphate-buffered saline (PBS), harvested with 0.25% trypsin/1 mM ethylenediaminetetraacetic acid (Gibco) and replated at 100 cells/cm^2 in CCM. Media are changed every 3-4 days. Sub-confluent cells (≤70% confluent) between passage 2 and passage 6 are used for all experiments as subsequent passages could affect pluripotent properties of ASCs.

2.3 Bioink Preparation

0.3 g of Gelatin (Type B, Sigma-Aldrich, St. Louis, MO, USA) is first dissolved in 10 ml of water (HyClone™ Water, GE Healthcare Life Sciences). The covered glass beaker is maintained at ~40°C while being magnetically stirred. On gelatin dissolution, 0.3 g of sodium alginate (Sigma-Aldrich, St. Louis, MO, USA) is added to the solution and mixed for at least 6 h to prepare the gelatin-alginate hydrogel. 8×10^6 cells are suspended in 200 µL of CCM and mixed with 4 ml of hydrogel for 5 min in the beaker using a magnetic stirrer to obtain a uniform distribution of cells (2×10^6 cells/ml) in the gelatin-alginate bioink. The bioink is then transferred to a 3 ml syringe barrel attached with 22G or 410 µm internal diameter tips before bioprinting. To prepare a bioink with the incorporation of glass, 0.06 g of 13-93B3 glass (10 wt% of hydrogel material) is added to the gelatin solution and stirred to obtain uniform suspension of glass particles. Sodium alginate is then added to the solution and stirred to obtain the Alg-Gel-glass hydrogel. ASCs suspended in CCM are first hand-mixed in gel and later magnetically stirred for no more than 5 min to obtain a uniform distribution of the ASCs in the bioink.

2.4 Scaffold Fabrication

Scaffolds are fabricated using a 3D printer (Geeetech, Prusa I3 A Pro) modified to have two syringes connected to external digital syringe dispensers (Loctite®, Rocky Hill, CT, USA) that are computer controlled. A bioprinter schematic is shown in Figure 1A, a printing schema is illustrated in Figure 1B, and the bioprinter set-up inside a laminar flow hood is shown in Figure 1C. Scaffolds measuring 12 × 12 × 1 mm^3 are fabricated with 0-90° filament orientation in alternate layers. A customized software is written to generate the G-code and control the printing process. Air pressure of 40 psi is used to extrude the PCL and PCL/13-93B3 pastes and 4 psi is found to be suitable for the bioink extrusion. A layer height of 0.1 mm and a printing speed of 10 mm/s are used to fabricate polymer scaffolds, and a height of 0.2 mm and a speed of 15 mm/s are used to fabricate bioink scaffolds. A filament spacing of 0.7 mm is used to fabricate PCL and PCL/13-93B3 scaffolds for scaffold characterization, and a spacing of 2.5 mm is used for bioprinting. For bioprinting, filaments are deposited in 0° direction twice followed by one layer of bioink extrusion as shown in Figure 1B, which is done to allow enough shrinkage and swelling of the bioink in between the polymer-glass composite filaments. A dwell time of 30 s is used after each layer to allow filament drying before deposition of subsequent layers. The bioink syringe is kept in the incubator maintained at ~37.5°C for ~5 min before bioprinting. The bioprinting process is carried out at room temperature inside the laminar flow hood following sterile practices.

2.5 Scaffold Characterization

PCL and PCL/13-93B3 scaffolds measuring 10 × 50 × 1 mm^3 are fabricated for assessment of mechanical properties. A sample size of n=10 is used for tensile tests using an Instron machine (Instron 5969, Norwood, MA, USA). One-way ANOVA is performed in Minitab and the resulting difference in means is considered significant if P<0.05. Optical microscopic images are used to measure the filament width and pore sizes with at least 10 measurements and the results are reported as average ± standard deviation. Scaffolds are dried, weighed, and soaked in Dulbecco's Modified Eagle Medium (DMEM) (Gibco) with a weight: volume ratio of 1:200 (g: ml) in high-density polyethylene bottles and kept in an incubator maintained at 37°C. After soaking for up to 28 days in DMEM, the scaffolds are dried overnight, coated with Au-Pd and observed under a scanning electron microscope (SEM) (S-4700, Hitachi, Japan) to analyze the surface morphology and formation of hydroxyapatite (HA)-like crystals on the surface.

2.6 Cell Viability

A live/dead viability kit (ThermoFisher, Carlsbad, CA, USA) is used to assess the cell viability according to the manufacturer's instructions. After 1 day and 7 days, the scaffolds are washed with PBS and are stained with 1 ml of prepared reagents (Calcein AM to stain live cells and Ethidium homodimer-1 to stain dead cells) for 30 min at room temperature and examined under a confocal microscope (Nikon A1R-HD Eclipse Ti2, Melville, NY, USA). Three scaffolds are examined per experimental group, and images are taken covering an area of 6 × 6 mm^2. Cell viability is calculated as: (live cells/total cells) × 100%. The maximum intensity projection images are quantified using ImageJ software and the difference in means is considered significant if P<0.05 based on the one-way ANOVA performed in Minitab.

3. Results and Discussion

3.1 Scaffold Fabrication and Physical Assessment

For scaffolds fabricated without the bioink, PCL/glass composite scaffolds had a filament width of 328±36 µm

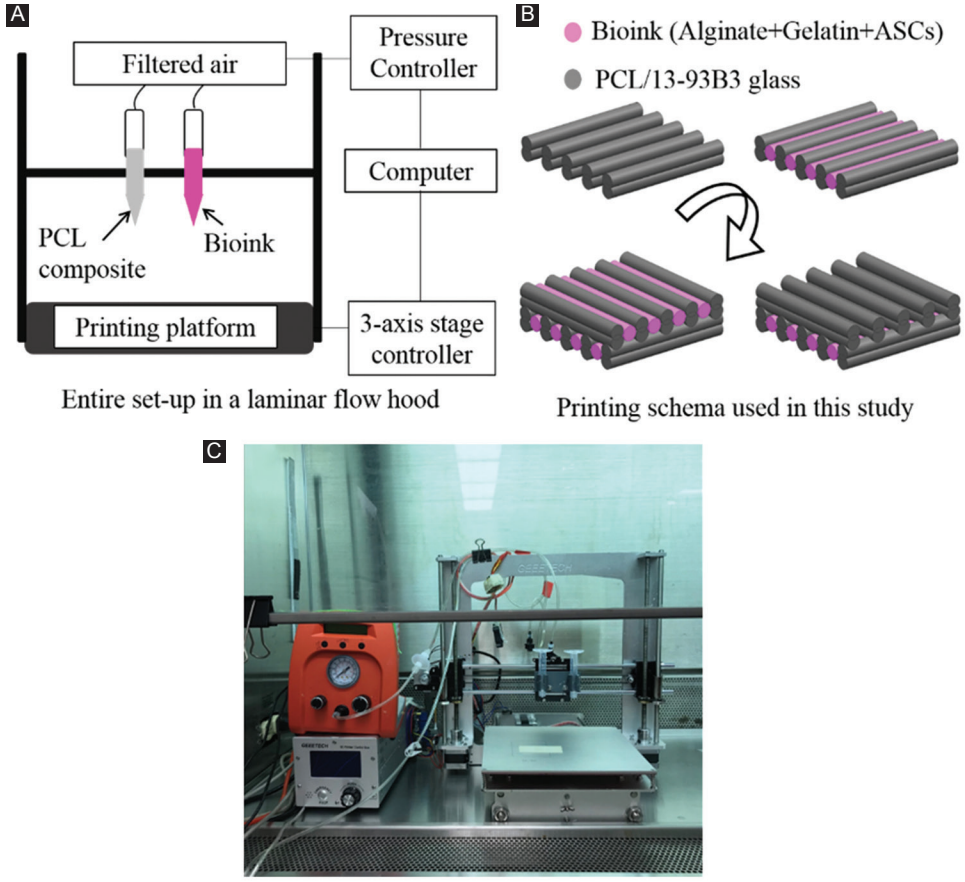

Figure 1. Solvent-based extrusion bioprinting process: (**A**) Schematic of the bioprinter, (**B**) schematic of the printing process, and (**C**) bioprinter set-up in a laminar flow hood.

and pore size of 314±22 µm, and the PCL scaffolds had a filament width and pore size of 340±19 µm and 305±18 µm, respectively. The target was to achieve a scaffold pore size of ~300 µm, which is a typical pore size recommended for bone repair and regeneration[26]. With a printer accuracy of ±10 µm, the results are considered satisfactory for investigating bioactive glass and its effects on scaffold properties and cell viability in this study. Figure 2A shows the optical microscopic images of filaments and pores, and the scaffolds fabricated for tensile tests. To measure the swelling of the Alg-Gel hydrogel, fabricated scaffolds measuring 12 × 12 × 0.6 mm^3 were cross-linked using 0.3 M $CaCl_2$ for 10 min, washed with PBS, and soaked in DMEM for 24 h. An average area shrinkage of ~30% was observed in all Alg-Gel scaffolds immediately after cross-linking, and they swelled by ~12% after 24 h in comparison to their nominal dimensions. The scaffolds increased in weight by ~45% after 24 h in comparison to their weight immediately after cross-linking. Scaffolds fabricated with Alg-Gel and PCL/glass+Alg-Gel are shown in Figure 2B along with the tensile testing of the cross-linked Alg-Gel scaffolds. The ultimate tensile strength, yield strength, and elastic modulus values of the samples are given in Table 2. Typical stress-strain curves are representing that the average values are plotted in Figure 2C, where the curve for Alg-Gel almost overlaps the X-axis. The results indicate an increase in scaffold brittleness with the addition of 13-93B3 glass (in 50 wt%). The yield strength of the PCL/glass composite is higher than the PCL polymer, and the maximum strength of the polymer is higher than the composite. Another clear indicator of brittleness for the PCL/glass is the significant increase in elastic modulus and its composite behavior in fracture (Figure 2C).

The mechanical properties of Alg-Gel hydrogel scaffolds are significantly less in comparison to the polymer or composite scaffolds. Nevertheless, the values are in a similar range in terms of tensile strength and elastic modulus values reported in other studies with Alg-Gel hydrogels[27,28]. The mechanical properties of bioprinted PCL+Alg-Gel scaffolds are also significantly less than PCL or PCL/glass scaffolds fabricated by this method. This is because the PCL and PCL/glass scaffolds were completely dried before mechanical tests, whereas the PCL+Alg-Gel scaffolds did not dry completely

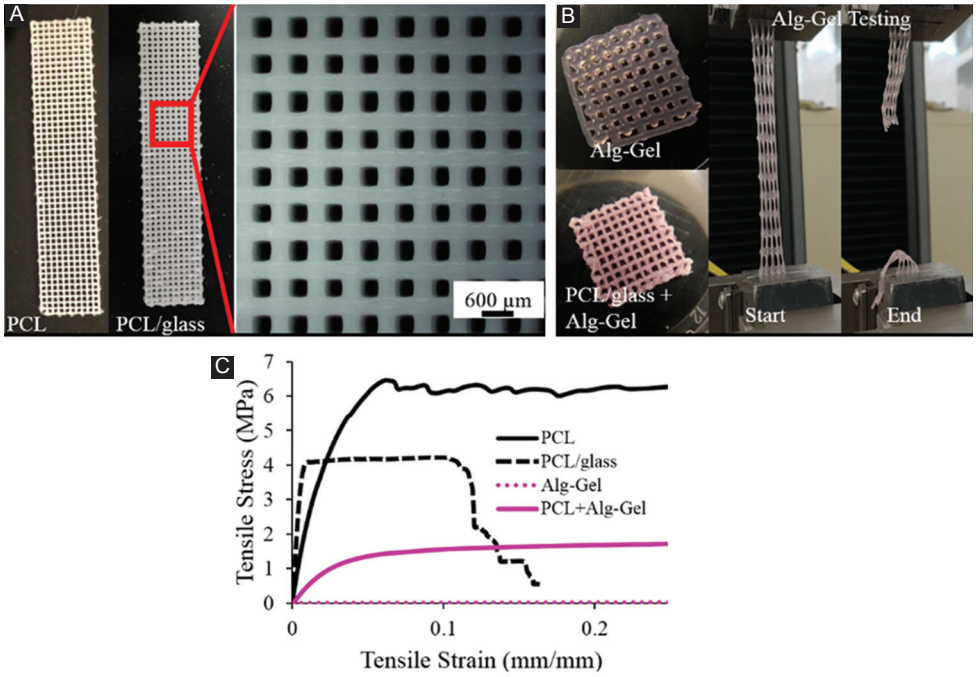

Figure 2. Scaffold fabrication with solvent-based three-dimensional bioprinting: (**A**) Mechanical testing specimens fabricated with polycaprolactone (PCL) and PCL/glass with an optical microscopic images showing the filaments and pores, (**B**) alginate-gelatin (Alg-Gel) scaffold and PCL/glass+Alg-Gel scaffolds and tensile testing of Alg-Gel scaffolds, (**C**) typical stress-strain graphs of all samples in this study.

Table 2. Scaffold's mechanical properties (in MPa).

Property\sample	PCL	PCL/glass	Alg-Gel	PCL + Alg-Gel
Maximum tensile strength	6.8 ± 0.9	4.4 ± 0.4	0.24 ± 0.1	1.8 ± 0.3
Yield strength	2.9 ± 0.5	3.8 ± 0.4	0.09 ± 0.01	0.7 ± 0.2
Elastic modulus	263.9 ± 19.2	733.9 ± 96.8	0.3 ± 0.1	50.6 ± 14.3

PCL: Polycaprolactone, Alg-Gel: Alginate-gelatin

during their fabrication as the filaments were surrounded by wet Alg-Gel and the scaffold was immediately cross-linked by submerging them in $CaCl_2$ solution after fabrication. Despite this, the PCL+Alg-Gel scaffold properties show significant improvement in comparison to the Alg-Gel scaffold as listed in Table 2. Unlike the melt-deposition process that requires a high temperature to extrude pastes of polymer-glass composites and thus making it unfeasible for bioprinting, the solvent-based extrusion method enables bioprinting with polymer-glass composites and hydrogels. The solvent-based process also significantly improves the scaffold properties in comparison to hydrogel only scaffolds.

3.2 Scaffold Weight Loss and Bioactivity

Our motivation to add 13-93B3 glass to the polymer matrix in this study is to introduce the bioactive ionic micronutrients released with 13-93B3 glass dissolution in the 3D cell culture environment. Previous reports show that 13-93B3 glass bonds to both hard and soft tissues, and regenerates good quality tissue in wound healing applications without forming scar tissue[25,29-31]. These studies have shown that 13-93B3 glass converts to apatite crystals on the scaffold surface and has a very fast dissolution rate (between a few hours and days). In the current study, as glass is dispersed in the highly viscous polymer-solvent paste, it is important to analyze two different aspects of the fabrication: (i) The glass particle distribution in the polymer matrix and (ii) the glass dissolution over time in the DMEM solution.

To investigate the glass particle distribution in the paste, a tub of PCL/glass paste was made and transferred to a syringe and scaffolds measuring 12 × 12 × 0.5 mm^3 were fabricated exhausting the entire paste in the syringe. One tub of paste provided on an average between 13 and 15 scaffolds. The individually labeled scaffolds 1-15 were dried, weighed, and soaked separately in DMEM for 2 weeks to measure the weight loss. The experiment was repeated 4 times, and the weight loss percentage difference between scaffolds numbered from 1 to 15 was found to be not statistically significant (P>0.05). Since a non-uniform glass particle distribution would provide significant

differences in scaffold weight loss measurements, the result of no difference in the percentage scaffold weight loss from scaffold #1-#15 indirectly proves that the glass particles are uniformly distributed. Second, to investigate the glass dissolution, the fabricated PCL/glass scaffolds were soaked in DMEM and kept in an incubator maintained at 37°C to simulate the conditions of ASCs in bioprinted scaffolds. Scaffolds were weighed at different time intervals to record the weight loss percentages. The weight loss graphs of PCL and PCL/glass scaffolds are shown in Figure 3A. The PCL/glass scaffolds show a maximum weight loss percentage of ~31%, which is very close to the theoretical weight loss of 32% assuming the entire 13-93B3 glass in the scaffold either dissolves or forms HA crystals on the surface. The weight loss percentage of PCL scaffolds is <3% over a period of 28 days and is in agreement with the reports in literature which discussed the slow degradation rate of PCL[32]. The SEM images of the PCL/glass scaffold cross-sections on day 0 and day 14 are shown in Figure 3B. Some of the bigger glass particles in the PCL/glass matrix are pointed with arrows in the figure. The cross-section on day 14 clearly shows higher porosity and fewer glass particles, indicating the dissolution of a majority of glass particles. The SEM images of the scaffold surface show fine microcracks (pointed with arrows) on the scaffold surface on day 0 and the presence of HA-like crystal formations on the surface on day 14. The X-ray diffraction (XRD) results in Figure 3C show peaks indicating the formation of non-stoichiometric HA, which is consistent with the previous studies where PCL/13-93B3 glass scaffolds showed similar HA-like conversion but the energy-dispersive X-ray spectroscopy results also confirmed the presence of Ca, P, and O elements on the surface[6].

3.3 Cell Viability

For a 3D bioprinting process, it is crucial to determine the cell viability in a bioink before determining the overall cell viability when the bioink is extruded with PCL or PCL/glass material. For this, ASCs viability in the bioink described in Section 2.3 and their survivability through the bioprinting process was quantified using the live/dead assay. The viability was evaluated immediately after fabrication and cross-linking with 0.3 M $CaCl_2$ solution for 10 min. The bioink only scaffolds provided cell viability of 81±9%, which is well within the range of 70-90% reported in other studies with Alg-Gel hydrogel using different cell types including ASCs at

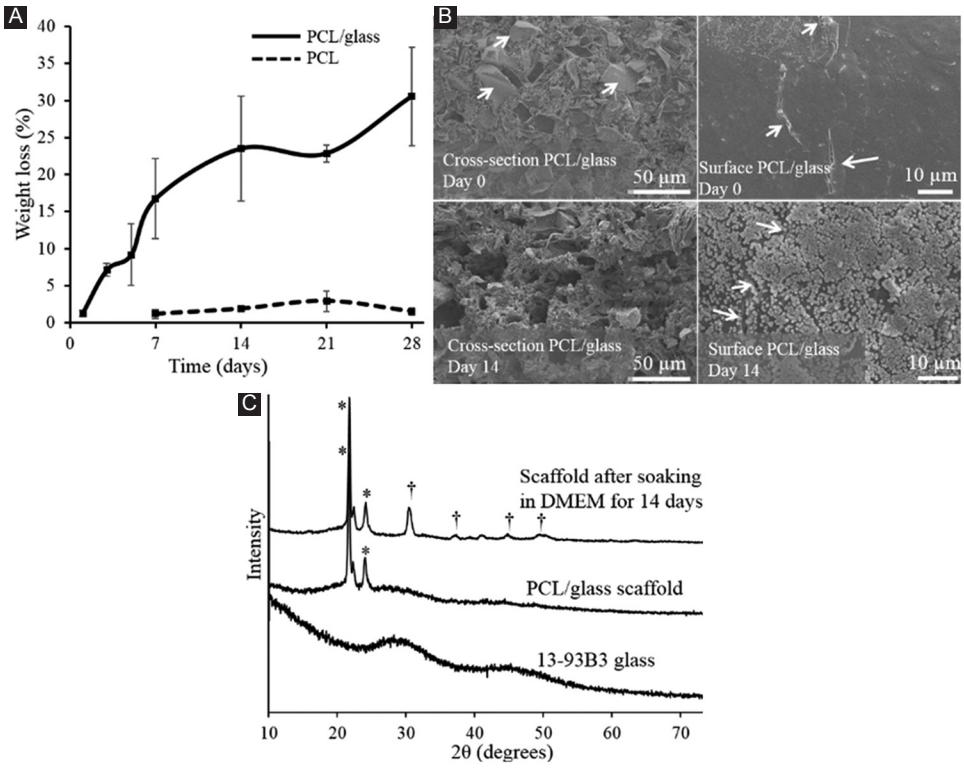

Figure 3. (**A**) Weight loss curves of polycaprolactone (PCL) and PCL/glass scaffolds indicating glass dissolution, (**B**) scanning electron microscope images of PCL/glass scaffold showing cross-section and surface morphology immediately after fabrication and after 14 days in Dulbecco's Modified Eagle Medium (DMEM); arrows show glass particles in the cross-section and microcracks on the scaffold surface; scaffolds are shown with hydroxyapatite-like crystal formations on the surface, (**C**) X-ray diffraction curves of as-received materials, fabricated scaffolds, and after soaking in DMEM for 14 days; *indicates semi-crystalline peaks of PCL and †indicates unknown peaks.

different cell concentrations[33-35]. We consider this as the baseline metric for ASC viability in the Alg-Gel scaffold fabricated using our process. To investigate the effect of 13-93B3 glass on cell viability, the glass was added in two different approaches: (i) Indirect – glass is added to PCL matrix, and bioink filaments are extruded in between PCL/glass filaments thus making ASCs contact with glass indirect, and (ii) direct – glass is added to the bioink to achieve a direct contact between ASCs and glass particles. ASCs viability was studied in both of the above cases by performing live/dead assay after 1 day and 7 days.

3.3.1 Indirect Glass Addition

In this approach, as 13-93B3 glass dissolves from the PCL matrix, the ionic dissolution products that are physiologically relevant micronutrients for human body are released to the surrounding Alg-Gel environment with ASCs. Figure 4 shows the representative maximum intensity projections of the multiple Live/Dead images taken at a Z-interval of 40 µm using a confocal microscope. The green fluorescent spots indicate live cells and the red fluorescent spots indicate dead cells. Overall, for all scaffold types, the results indicate more live cells in comparison to dead cells. Figure 5 shows the quantification of Live/Dead assay results. A non-uniform distribution of dead cells along the scaffold thickness was noticed with a relatively high percentage of dead cells located in the lower scaffold (LS) region than the rest of the scaffold (ROS) region. A majority of dead cells in the images (Figure 4) were observed in the LS region, which was measured from the scaffold bottom in contact with the glass Petri dish to 0.1 mm in Z-height. Figure 5B shows a comparison plot of cell viability in the LS region to the ROS region.

A relatively high percentage of viable ASCs in the ROS region in comparison to the LS region for all scaffold types can be clearly observed in the plot. There could be two possible explanations for this result: (i) Standoff distance of the tip during fabrication and (ii) hypoxic-like conditions in the scaffold bottom (LS region). The standoff distance used to extrude the first layer of bioink was 0.1 mm for all scaffold types. A small standoff distance might have caused additional backpressure on cells in the bioink at the bottom region causing cell death. To verify this, the bioink was extruded at a larger standoff distance (1 mm) as a spherical shaped specimen. Live/dead assay analysis on the specimen indicated no significant differences in the percentage of dead cells between the LS and ROS regions. The second possible reason could be the lack of CCM circulation in the bioink extruded between PCL and PCL/glass filaments that are surrounded by relatively dense polymeric filaments in static culture conditions. Despite being surrounded by the polymer filaments, ASCs in bioink in the top region have accessible CCM. One possible solution to avoid low viability in the LS region that was not considered in this study could be incubating scaffolds on top of transwell

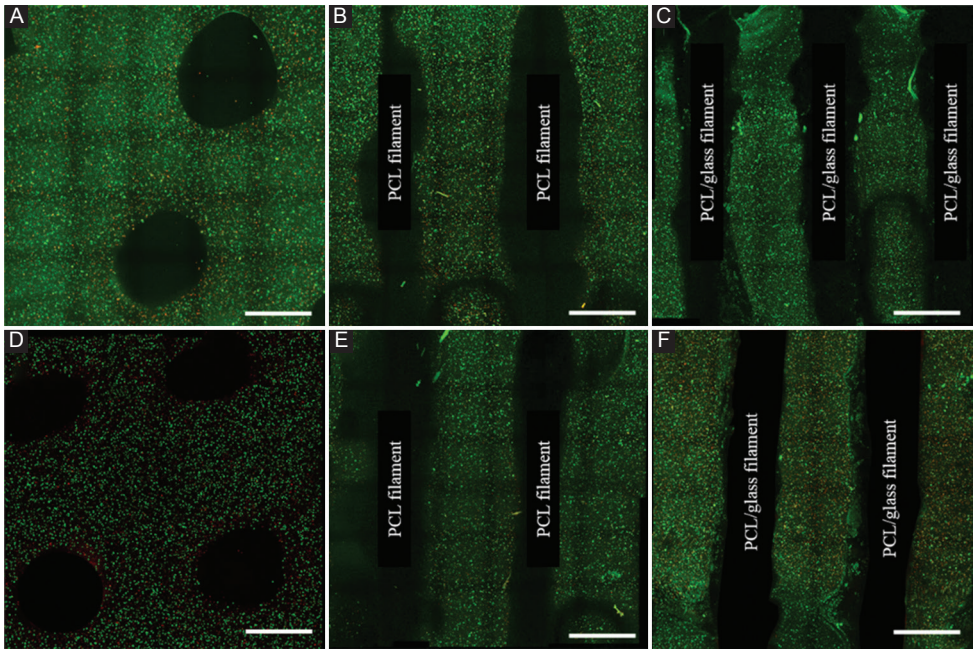

Figure 4. Live/dead images showing the viability of ASCs in the alginate-gelatin bioink (scale bar: 1 mm). (**A, B, C**) After 1 day and (**D, E, F**) after 7 days incubation, (**A, D**) bioink, (**B, E**) polycaprolactone (PCL)+bioink, and (C,F) PCL/glass+bioink. Day 1 images showed good and viable ASCs with few dead cells in all scaffolds, but cell viability reduced after 7 days of incubation, especially, to ~50% in the PCL/glass+bioink.

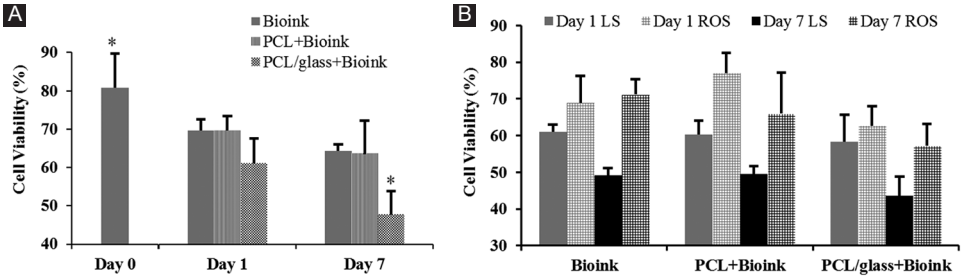

Figure 5. Cell quantification using live/dead assay analysis: (**A**) Cell viability in bioink immediately after cross-linking compared to viability in scaffolds fabricated in different configurations after 1 day and 7 days in culture and (**B**) cell viability split up between the lower scaffold region (0-0.1 mm from the scaffold bottom) and the rest of the scaffold.

inserts where pores could enable CCM circulation to the LS region.

The results also indicate a reduction in cell viability in all scaffold types after day 7 and even more significant reduction in the PCL/glass+bioink scaffold ($P<0.05$). The overall decrease in cell viability could be understood by considering the two different aspects: (i) The stability of Alg-Gel hydrogel and (ii) the effect of the environment due to PCL and PCL/glass filaments. The cell viability in the Alg-Gel hydrogel decreased from 81% to 64% on day 7, and the reason for reduced viability in Alg-Gel could be linked to the stability of the Alg-Gel hydrogel. The composition of hydrogel used in this study contains both gelatin and alginate in a 1:1 ratio. The cells are mixed in the hydrogel, and scaffolds are bioprinted and cross-linked with 0.3M $CaCl_2$ solution for 10 min, all at room temperature. The calcium ions crosslink the alginate and it was expected that the gelatin would be contained in the cross-linked scaffold. However, in the culture conditions at 37°C incubation, gelatin present in the scaffold could transform into liquid phase and leach out into the media. To test this, scaffolds without cells were fabricated, incubated at 37°C in DI water, and the DI water was tested for the presence of gelatin using proton nuclear magnetic resonance (^{1}H-NMR) spectroscopy. Figure 6 shows the ^{1}H-NMR spectra of the DI water collected after 1 day and 7 days of incubation in comparison to the reference spectra of dissolved gelatin in DI water. The highlighted region shows typical peaks in the spectra that correspond to gelatin. It can be clearly observed that DI water collected after 7 days contains gelatin while it could be either in insufficient amounts to detect or not present after 1-day incubation in the absence of no matching peaks in the 1-day sample. The decrease in viability could be linked with the gelatin release from the Alg-Gel hydrogel as studies in the past have indicated that alginate alone cannot support the mammalian cell adhesion and proliferation due to the lack of Arginine-Glycine-Aspartate (RGD) tripeptide[36,37]. Our future work will include crosslinking gelatin along with

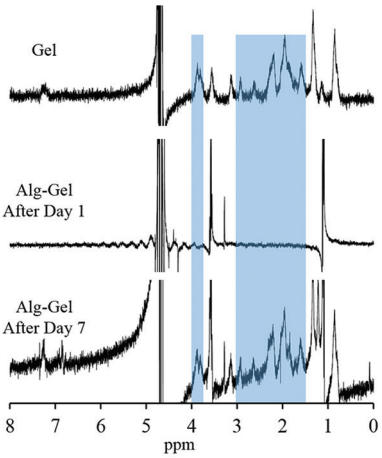

Figure 6. Proton nuclear magnetic resonance spectra from sample DI water (0.6 ml) taken from alginate-gelatin (Alg-Gel) hydrogel samples incubated in DI water at 37°C with 5% CO_2 after 1 day and 7 days. No gelatin peaks were observed in 1-day sample but peaks matched with reference gelatin solution (gel) for the 7-day sample. The additional sharp peaks in Alg-Gel samples refer to unsuppressed water and ethanol.

alginate to provide a hydrogel that is both cell-friendly and has sufficient structural integrity.

The second aspect to analyze the decreased cell viability in all scaffold types after 7 days in culture lies in the environment change due to simultaneous extrusion of PCL and PCL/glass filaments along with bioink. In Figure 5A, it can be clearly observed that the cell viability in PCL+bioink scaffolds remained identical to that of bioink scaffolds in the same incubation time indicating that there is no effect on viability with the extrusion of PCL filaments. Therefore, it can be concluded that the solvent-based extrusion process is a viable alternative method to fabricate cellularized scaffolds with polymer supporting filaments. It is expected that the viability of cells in bioink will decide the overall cell viability in PCL+bioink scaffolds. However, cell viability in PCL/glass+bioink scaffolds is significantly lower in comparison to bioink and PCL+bioink scaffolds. The

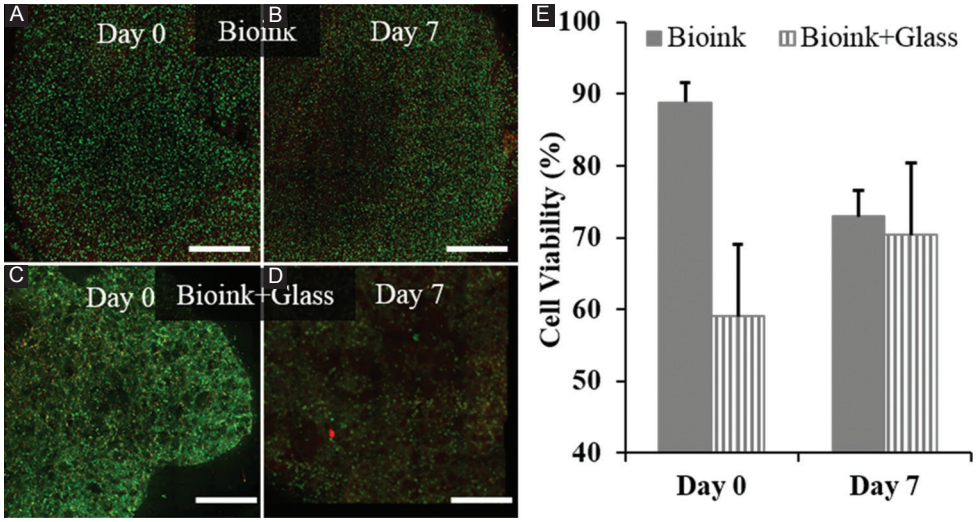

Figure 7. Live/dead images showing the viability of human adipose-derived mesenchymal stem cells (ASCs) in spheroid-like samples (scale bar: 1 mm): (**A, B**) bioink, (**C, D**) bioink+glass, (**A, C**) immediately after crosslinking (day 0), and (**B, D**) after 7 days (**E**) ASC viability on day 0 and day 7. The bioink shows a relatively higher percentage of viable ASCs (green) with increased dead cells (red) after 7 days in culture. Bioink+glass samples on day 0 had more dead cells (viability - 59%) and exhibited high background noise (green) due to borate ions, which reduced after 7 days in culture (with glass dissolution and media changes).

viability in PCL/glass+bioink scaffolds is decreased even further due to the 13-93B3 glass effects over and above the decrease caused due to bioink stability, as explained earlier. The borate network of 13-93B3 glass is chemically not as durable as silicate network of Bioglass® (45S5 glass) and therefore dissolves at a faster rate in aqueous media. Such faster glass dissolution resulted in a pH increase of the CCM that could potentially harm cells in the bioink. As 13-93B3 glass dissolves, the ionic products are released into the surrounding environment from the PCL/glass filaments as the scaffold loses almost 16% weight after 7 days (Figure 3A). The weight loss experiments with PCL/glass scaffolds (without cells) in static conditions increased the pH up to 8.8 (from a neutral pH 7-7.4) within one week without the replacement of DMEM. The bioprinted PCL/glass+bioink scaffolds were incubated in 5 ml CCM in comparison to 20 ml DMEM used to soak PCL/glass scaffolds for weight loss experiments. This resulted in a high ionic concentration with 13-93B3 glass dissolution in small volumes and a drastic pH increase that could be the reason for low cell viability in PCL/glass+bioink scaffolds. Despite replenishing PCL/glass+bioink scaffolds with new CCM every 3 days, the pH could still be relatively high near the locations surrounding PCL/glass filaments due to insufficient media circulation to bioink surrounded by PCL/glass filaments in static conditions. In addition, the concentration of 13-93B3 glass used in the current study is very high (~45 mg per PCL/glass+bioink scaffold or ~9 mg/ml in concentration) in comparison to other studies where stem cells are exposed to very low concentrations of silicate-based glasses ranging from 0.6 to 2.5 mg/ml[38,39]. It was reported that concentrations above 1 mg/ml have significantly hampered stem cells functions. The results from our current study also indicate that a faster dissolving glass such as 13-93B3 (compared to silicate-glasses) and at high concentrations could damage ASCs rather than stimulate them and initiate favorable phenotypic changes with the released ionic micronutrients. Dynamic culture conditions with a low concentration of 13-93B3 glass (<2.5 mg/ml) could be more suitable for bioprinting with PCL/13-93B3 glass composite and will be pursued in the future.

3.3.2 Direct Glass Addition

The direct mixing of 13-93B3 glass with Alg-Gel hydrogel and the effect of glass on ASCs were also investigated. After the addition of 13-93B3 glass to the gelatin solution, the finer glass particles dissolved rapidly, causing an increase in the pH (to >8 from 7.4). The release of Ca^{2+} and other ions from the glass aided in initiating the alginate crosslinking in the course of hydrogel preparation. The viscosity of the Alg-Gel-glass mixture changed rapidly within 1 h, unlike overnight stirring that was required for the Alg-Gel solution. After ASCs were mixed uniformly in the hydrogel, the bioink was extruded in a 6-well plate at a standoff distance of 5 mm to form spheroid-like samples (~5 mm in diameter). The samples were immediately cross-linked, and cell viability was analyzed using a Live/Dead assay kit. Figure 7 shows the Live/Dead images of the bioink and bioink+glass spheroids immediately after cross-linking and after 7 days in culture. The bioink spheroids (Figure 7A) had a cell viability of 89±3% immediately after crosslinking

and their viability on day 0 is comparable to bioink scaffolds fabricated in the indirect glass addition approach on day 0 (81±9%). The cell viability in bioink spheroids after 7 days (Figure 7B) decreased significantly to 73±4% after 7 days in culture (Figure 7E) although the percentage was relatively higher than the 3D printed bioink scaffold after 7 days (64±2%). However, it has to be noted that the cell viability in the ROS region of 3D printed bioink scaffold (71±4%) was similar to the bioink spheroids with no statistically significant difference. The difference in overall viability is due to the low viability in the bottom layers of the 3D printed scaffold and lack of media circulation that does not arise in small volume spheroid culture.

For the bioink+glass spheroids, the results indicated toxicity with the direct glass addition to Alg-Gel hydrogel at 6 mg/ml of gel concentration. Figure 7C and D shows the live/dead images of the bioink+glass spheroid-like specimens on day 0 and after 7 days in culture, respectively. A high background noise (green) from glass particles was noticed while imaging bioink+glass specimens on day 0. A similar green fluorescence was observed in filaments while culturing cells on PCL/13-93B3 composite scaffolds[40]. This is due to the interference of the borate ions from the 13-93B3 glass with the calcein acetoxymethyl compound present in the live/dead reagents. ImageJ software was used to remove the smaller pixels representing the glass particle background before quantifying the live and dead cells. Bioink+glass spheroids had low ASC viability of 59±6% on day 0 due to the pH increase. Despite the initial pH shock and cell death, the ASC viability improved to 70±5% after 7 days in a culture which could be due to pH improvement as the environment becomes closer to neutral pH due to changing media every 2-3 days. The background noise observed on day 0 was greatly reduced in samples after day 7 (Figure 7D), which also indirectly indicates the glass dissolution and concentration reduction process. Even as the cell viability is low after 7 days in culture, there was no significant difference between cell viability in bioink and bioink+glass spheroids.

The viability of ASCs in 3D cell cultures in the presence of 13-93B3 glass was investigated in this study. The 13-93B3 glass was introduced in two different approaches, and the overall volumetric glass concentration is slightly different in the two approaches (9 mg/ml in indirect approach and 6 mg/ml direct approach). In both approaches and at such glass concentrations, toxicity was observed with glass mainly due to pH shock. In a recent study, Thyparambil *et al*. investigated the effects of 13-93B3 glass on phenotypic changes in ASCs in 2D cell cultures[41]. The experiments were performed in a similar fashion comparable to those by researchers who investigated effects of silicate glasses on human stem cells which involves loading cells on inserts and adding glass mixed CCM to the bottom of Petri dish[38,39]. The results indicated that at concentrations of 2.5 mg/ml for 13-93B3 glass and <1 mg/ml for silicate-based glasses provide optimum viability, differentiation, and migration of ASCs. Wang *et al*. reported the addition of SiO_2-CaO-P_2O_5 glass (5 mg/ml of gel) to Alg-Gel hydrogel improved proliferation and mineralization of osteogenic sarcoma cells[19]. However, the cell types are different to make a comparison with our current study. The results from our study evidently suggest that higher concentrations of faster degrading 13-93B3 glass rather than the slower degrading silicate glasses used by other researchers could have affected the viability of ASCs. A drastic pH change (pH shock) in addition to static culture conditions further diminished the viability.

The main outcomes from the current study are: (i) The proposed solvent-based bioprinting approach does not affect the viability of cells over and above the cell viability provided by the bioink as seen in indirect approach, (ii) viability of ASCs in bioink+glass spheroids increased after 7 days in culture and even higher than that of PCL/glass+bioink scaffold after 7 days (indirect approach), and (iii) viability of ASCs in bioink+glass spheroids increased whereas viability decreased in bioink spheroids. These results indicate that direct glass addition could possibly improve the feasibility of the Alg-Gel hydrogel as a bioink by aiding in crosslinking and slowing down gelatin degradation. There are reports that show crosslinked gelatin with silicate nanoparticles and stabilized gelatin molecular structure with sodium ions[42,43]. 13-93B3 glass and most of the dissolvable bioactive glasses release sodium ions as they dissolve and this could affect the Alg-Gel molecular structure. The rheological property of the Alg-Gel hydrogel with the addition of bioactive glasses is a current work in progress. We will also utilize lower concentrations of 13-93B3 glass in our future work and dynamic culture conditions (or bioreactors) to control the pH and release of physiologically relevant and important ionic micronutrients from borate bioactive glass to stimulate human primary cells in 3D environments *in vitro*. The importance of boron ions *in vivo* is very well established in wound repair, and so is the importance of bioactive glasses and their dissolution products in angiogenesis[44]. The micronutrients released by bioactive glasses stimulate growth factors such as VEGF and our current work is an attempt towards establishing the parameters that are required to create vascularized 3D cell cultures with human primary cells and bioactive glasses.

4. Conclusions

This study investigated the feasibility of bioprinting ASCs with highly resorbable, fast reacting, and highly angiogenic borate bioactive glass (13-93B3) using two

different approaches. In the first approach, a solvent-based extrusion 3D printing technique is used where PCL/13-93B3 composite (with 50 wt% glass) scaffolds are fabricated to provide controlled release of glass and bioactivity in a controlled fashion. Even as PCL/glass + bioink scaffolds have improved mechanical properties, the cell viability was decreased due to the high glass concentration and static culture conditions used in this study. The PCL + bioink scaffolds provided same cell viability as bioink scaffolds demonstrating the process feasibility. Alg-Gel hydrogel was utilized as a bioink for bioprinting, and it provided a uniform distribution of ASCs with good cell viability (>80%) immediately after fabrication which decreased to less than 70% after 7 days in culture due to unstable molecular structure. In the latter approach, glass is directly mixed with Alg-Gel hydrogel to create bioactive bioinks. Results indicated low cell viability with the direct glass addition due to the initial pH shock but could be promising in long-term 3D culture with improved ionic crosslinking of Alg-Gel hydrogel and cell viability. Overall, the results show the feasibility of the solvent-based 3D bioprinting technique for tissue engineering applications and the importance of bioactive glass concentrations to achieve viable 3D cell cultures.

Acknowledgment

The glass used in this study was provided by MO-SCI Corporation, Rolla, MO, USA. The authors also acknowledge the help provided by Apurv Saxena with NMR analysis.

Conflicts of Interest and Funding

No conflicts of interest were reported by the authors. This research is funded by the Intelligent Systems Center and the Center for Biomedical Research at the Missouri University of Science and Technology.

References

1. Moroni L, Boland T, Burdick JA, *et al*., 2018, Biofabrication: A Guide to Technology and Terminology. *Trends Biotechnol*, 36(4):384-402. DOI 10.1016/j.tibtech.2017.10.015.
2. Ozbolat IT, Hospodiuk M, 2016, Current Advances and Future Perspectives in Extrusion-based Bioprinting. *Biomaterials*, 76:321-43. DOI 10.1016/j.biomaterials.2015.10.076.
3. Pati F, Gantelius J, Svahn HA, 2016, 3D Bioprinting of Tissue/Organ Models. *Angew Chemie Int Ed*, 55(15):4650-65. DOI 10.1002/anie.201505062.
4. Choudhury D, Anand S, Naing M, 2018, The Arrival of Commercial Bioprinters Towards 3D Bioprinting Revolution! *Int J Bioprinting*, 4(2):1-19. DOI http://dx.doi.org/10.18063/IJB.v4i2.139.
5. Derakhshanfar S, Mbeleck R, Xu K, *et al*., 2018, 3D Bioprinting for Biomedical Devices and Tissue Engineering: A Review of Recent Trends and Advances. *Bioact Mater*, 3(2):144. DOI 10.1016/J.BIOACTMAT.2017.11.008.
6. Murphy C, Kolan K, Li W, *et al*., 2017, 3D Bioprinting of Stem Cells and Polymer/Bioactive Glass Composite Scaffolds for Tissue Engineering. *Int J Bioprinting*, 3(1):54-64. DOI 10.18063/IJB.2017.01.005.
7. Guo SZ, Gosselin F, Guerin N, *et al*., 2013, Solvent-cast Three-Dimensional Printing of Multifunctional Microsystems. *Small*, 9(24):4118-22. DOI 10.1002/smll.201300975.
8. Kaur G, Dufour JM, 2012, Cell Lines: Valuable Tools or Useless Artifacts. *Spermatogenesis*, 2(1):1-5. DOI 10.4161/spmg.19885.
9. Ong CS, Yesantharao P, Huang CY, *et al*., 2018, 3D Bioprinting Using Stem Cells. *Pediatr Res*, 83(1-2):223-31. DOI 10.1038/pr.2017.252.
10. Tasoglu S, Demirci U, 2013, Bioprinting for Stem Cell Research. *Trends Biotechnol*, 31(1):10-9. DOI 10.1016/j.tibtech.2012.10.005.
11. Uccelli A, Moretta L, Pistoia V, 2008, Mesenchymal Stem Cells in Health and Disease. *Nat Rev Immunol*, 8(9):726-36. DOI 10.1038/nri2395.
12. D'Andrea F, De Francesco F, Ferraro GA, *et al*., 2008, Large-scale Production of Human Adipose Tissue from Stem Cells: A New Tool for Regenerative Medicine and Tissue Banking. *Tissue Eng Part C Methods*, 14(3):233-42. DOI 10.1089/ten.tec.2008.0108.
13. Casteilla L, Dani C, 2006, Adipose Tissue-derived Cells: From Physiology to Regenerative Medicine. *Diabetes Metab*, 32(5 Pt 1):393-401. DOI DM-11-2006-32-5-1262-3636-101019-200519820.
14. Wang Y, Yin P, Bian GL, *et al*., 2017, The Combination of Stem Cells and Tissue Engineering: An Advanced Strategy for Blood Vessels Regeneration and Vascular Disease Treatment. *Stem Cell Res Ther*, 8(1):194. DOI 10.1186/s13287-017-0642-y.
15. Apelgren P, Amoroso M, Lindahl A, *et al*., 2017, Chondrocytes and Stem Cells in 3D-Bioprinted Structures Create Human Cartilage *In Vivo*. *PLoS One*, 12(12):e0189428. DOI 10.1371/journal.pone.0189428.
16. Kim Y, Kang K, Yoon S, *et al*., 2018, Prolongation of Liver-specific Function for Primary Hepatocytes Maintenance in 3D Printed Architectures. *Organogenesis*, 14(1):1-12. DOI 10.1080/15476278.2018.1423931.
17. Kolesky DB, Truby RL, Gladman AS, *et al*., 2014, 3D Bioprinting of Vascularized, Heterogeneous Cell-laden

Tissue Constructs. *Adv Mater*, 26(19):3124-30. DOI 10.1002/adma.201305506.

18. Sasaki JI, Hashimoto M, Yamaguchi S, *et al*., 2015, Fabrication of Biomimetic Bone Tissue Using Mesenchymal Stem Cell-derived Three-dimensional Constructs Incorporating Endothelial Cells. *PLoS One*, 10(6):e0129266. DOI 10.1371/journal.pone.0129266.
19. Wang X, Tolba E, Schröder HC, *et al*., 2014, Effect of Bioglass on Growth and Biomineralization of SaOS-2 Cells in Hydrogel after 3D Cell Bioprinting. *PLoS One*, 9(11):e112497. DOI 10.1371/journal.pone.0112497.
20. Ojansivu M, Rashad A, Ahlinder AE, *et al*., 2019, Wood-based Nanocellulose and Bioactive Glass Modified Gelatin-alginate Bioinks for 3D Bioprinting of Bone Cells. *Biofabrication*, 11(3):35010. DOI 10.1088/1758-5090/ab0692.
21. Zhang J, Chen Y, Xu J, *et al*., 2018, Tissue Engineering Using 3D Printed Nano-bioactive Glass Loaded with NELL1 Gene for Repairing Alveolar Bone Defects. *Regen Biomater*, 5(4):213-20. DOI 10.1093/rb/rby015.
22. Jung SB, Day DE, 2011, Revolution in Wound Care? Inexpensive, Easy-to-use Cotton Candy-like Glass Fibers Appear to Speed Healing in Initial Venous Stasis Wound Trial. *Am Ceram Soc Bull*, 90(4):25-9. Available from: https://www.ceramics.org/ceramic-tech-today/revolution-in-wound-care-inexpensive-easy-to-use-cotton-candy-like-glass-fibers-appear-to-speed-healing-in-initial-venous-stasis-wound-trial. [Last accessed on 2019 Apr 29].
23. Jung S, 2010, *Borate Based Bioactive Glass Scaffolds for Hard and Soft Tissue Engineering*. Doctoral Dissertations. Available from: http://www.scholarsmine.mst.edu/doctoral_dissertations/2075. [Last accessed on 2019 Apr 29].
24. Food and Drug Administration, 2016, *Department of Health and Human Services*. Food and Drug Administration. Available from: https://www.etswoundcare.com. [Last accessed on 2019 Apr 29].
25. Lin Y, Brown RF, Jung SB, *et al*., 2014, Angiogenic Effects of Borate Glass Microfibers in a Rodent Model. *J Biomed Mater Res Part A* 102A:4491-9. DOI 10.1002/jbm.a.35120.
26. Karageorgiou V, Kaplan D, 2005, Porosity of 3D Biomaterial Scaffolds and Osteogenesis. *Biomaterials*, 26(27):5474-91. DOI 10.1016/j.biomaterials.2005.02.002.
27. Luo Y, Lode A, Akkineni AR, *et al*., 2015, Concentrated Gelatin/Alginate Composites for Fabrication of Predesigned Scaffolds with a Favorable Cell Response by 3D Plotting. *RSC Adv*, 5(54):43480-8. DOI 10.1039/C5RA04308E.
28. Shi L, Xiong L, Hu Y, *et al*., 2018, Three-dimensional Printing Alginate/Gelatin Scaffolds as Dermal Substitutes for Skin Tissue Engineering. *Polym Eng Sci*, 58(10):1782-90. DOI 10.1002/pen.24779.
29. Zhou J, Wang H, Zhao S, *et al*., 2016, *In vivo* and *in vitro* Studies of Borate Based Glass Micro-fibers for Dermal Repairing. *Mater Sci Eng C*, 60:437-45. DOI 10.1016/J.MSEC.2015.11.068.
30. Earl P, Stoecker W, Jung S, 2018, *Clinical Case Studies ETS Wound Care*. Available from: https://www.etswoundcare.com/clinical-case-studies.html. [Last accessed on 2019 Apr 29].
31. Gu Y, Huang W, Rahaman MN, *et al*., 2013, Bone Regeneration in Rat Calvarial Defects Implanted with Fibrous Scaffolds Composed of a Mixture of Silicate and Borate Bioactive Glasses. *Acta Biomater*, 9(11):9126-36. DOI 10.1016/j.actbio.2013.06.039.
32. Woodruff MA, Hutmacher DW, 2010, The Return of a Forgotten Polymer Polycaprolactone in the 21st Century. *Prog Polym Sci*, 35(10):1217-56. DOI 10.1016/j.progpolymsci.2010.04.002.
33. Lee H, Won Koo Y, Yeo M, *et al*., 2017, Recent Cell Printing Systems for Tissue Engineering. *Int J Bioprinting*, 3(1):27-41. DOI 10.18063/IJB.2017.01.004.
34. Rezaei S, Shakibaie M, Kabir-Salmani M, *et al*., 2016, Improving the Growth Rate of Human Adipose-derived Mesenchymal Stem Cells in Alginate/Gelatin Versus Alginate Hydrogels. *Iran J Biotechnol*, 14(1):1-8. DOI 10.15171/ijb.1185.
35. Li Z, Huang S, Liu Y, *et al*., 2018, Tuning Alginate-gelatin Bioink Properties by Varying Solvent and Their Impact on Stem Cell Behavior. *Sci Rep*, 8(1):8020. DOI 10.1038/s41598-018-26407-3.
36. Jeon O, Alsberg E, 2013, Photofunctionalization of Alginate Hydrogels to Promote Adhesion and Proliferation of Human Mesenchymal Stem Cells. *Tissue Eng Part A*, 19(11-12):1424-32. DOI 10.1089/ten.TEA.2012.0581.
37. Rowley JA, Madlambayan G, Mooney DJ, 1999, Alginate Hydrogels as Synthetic Extracellular Matrix Materials. *Biomaterials*, 20(1):45-53. DOI 10.1016/S0142-9612(98)00107-0.
38. Qazi T H, Hafeez S, Schmidt J, *et al*., 2017, Comparison of the Effects of 45S5 and 1393 Bioactive Glass Microparticles on hMSC Behavior. *J Biomed Mater Res A*, 105(10):2772-82. DOI 10.1002/jbm.a.36131.
39. Gholami S, Labbaf S, Houreh AB, *et al*., 2017, Long Term Effects of Bioactive Glass Particulates on Dental Pulp Stem Cells *In Vitro*. 3(1):97-103. DOI 10.1515/bglass-2017-0009.
40. Kolan K, Li J, Roberts S, *et al*., 2018, Near-field Electrospinning of a Polymer/Bioactive Glass Composite

to Fabricate 3D Biomimetic Structures. *Int J Bioprinting*, 5(1):1-6. DOI 10.18063/ijb.v5i1.163.

41. Thyparambil N, Bromet B, Gutgesell L, *et al*., 2019, *Borate Bioactive Glass Triggers Phenotypic Changes in Adipose Stem Cells*. Manuscript Submitted for Publication.
42. Patel RG, Purwada A, Cerchietti L, *et al*., 2014, Microscale Bioadhesive Hydrogel Arrays for Cell Engineering Applications. *Cell Mol Bioeng*, 7(3):394-408. DOI 10.1007/s12195-014-0353-8.
43. Xing Q, Yates K, Vogt C, *et al*., 2015, Increasing Mechanical Strength of Gelatin Hydrogels by Divalent Metal Ion Removal. *Sci Rep*, 4(1):4706. DOI 10.1038/srep04706.
44. Kargozar S, Baino F, Hamzehlou S, *et al*., 2018, Bioactive Glasses: Sprouting Angiogenesis in Tissue Engineering. *Trends Biotechnol*, 36(4):430-44. DOI 10.1016/j.tibtech.2017.12.003.